# DESIGN OF HIGH MECHANICAL PERFORMANCE CARBON NANOTUBE STRUCTURE: MACHINE-LEARNING ASSISTED HIGH-THROUGHPUT MOLECULAR DYNAMICS SIMULATION APPROACH

Go Yamamoto [1,2], Yi Xiang [3], Koji Shimoyama [4], and Keiichi Shirasu [5]

[1] Department of Aerospace Engineering, Tohoku University, Sendai, Japan, gyamamoto@tohoku.ac.jp, http://www.yamamotolab.mech.tohoku.ac.jp/
[2] School of Mechanical Engineering, Sungkyunkwan University, Suwon, Republic of Korea
[3] Department of Aerospace Engineering, Tohoku University, Sendai, Japan, xiang.yi.t3@dc.tohoku.ac.jp
[4] Ful Institute of Fluid Science, Tohoku University, Sendai, Japan, shimoyama@tohoku.ac.jp
[5] Department of Finemechanics, Tohoku University, Sendai, Japan, keiichi.shirasu.c1@tohoku.ac.jp

**Keywords:** Carbon nanotube, Molecular dynamics simulation, Mechanical properties, Machine learning, Frenkel-pair crosslink

## ABSTRACT

Multi-walled carbon nanotubes (MWCNTs) are novel materials with exceptional mechanical properties. In order to gain insight into the design of MWCNT-reinforced composite materials with high mechanical performance, this study determined the optimal structure of MWCNTs with high nominal tensile strength, where the nominal values correspond to the cross-sectional area of the entire specimen, including the hollow core. Machine learning based high throughput molecular dynamics (HTMD) simulation was used to investigate the relationship between the following structural parameters/properties: diameter, number of walls, chirality and crosslink density between walls. It was observed that the influence of crosslink density on the nominal tensile strength tends to decrease gradually from the outside to the inside; in general, the crosslink density between the outermost wall and its adjacent wall is highly significant. Under the calculation conditions, Armchair-type eight-walled nanostructures in which the chirality of the innermost tube was (8,8) and the crosslink densities were 1.01%, 0.93%, 1.14%, 0.92%, 0.84%, 1.08%, and 1.19% (from outside to inside) were found to be optimal, with the nominal tensile strength and Young's modulus reaching 57–59 GPa and 650–670 GPa, respectively.

## INTRODUCTION

Multi-walled carbon nanotubes (MWCNTs) with unique mechanical properties are considered to be a promising reinforcing agent for composite applications [1–3]. MWCNTs synthesized by the arc discharge method at high synthesis temperature often exhibit the sword-in-sheath type failure, because the tensile load applied to the MWCNTs is carried exclusively by the outermost wall due to its high crystallinity [4,5], while MWCNTs synthesized by the commonly used chemical vapor deposition (CVD) method are found to experience all-wall failure due to load transfer caused by structural defects [6]. For these reasons, both fracture modes result in a nominal tensile strength based on the cross-sectional area of the full specimen, i.e., the cross-section including the hollow core does not reach more than 10 GPa [7]. Thus, it is expected that there should be an optimal structure with a suitable number of detectors that can make the tube achieve high strength, and the understanding of the geometric properties of the optimal structure should have a positive influence on future work for tailoring structures of MWCNTs used as reinforcing agents in composite applications.

In this study, we investigate the relationship between geometrical parameters and mechanical properties of CNTs. To guide the design of CNT composites, we mainly focused on the nominal values of the mechanical properties of CNTs. We show that by combining molecular dynamics (MD) method and machine learning, it is possible to predict an optimized structure with specific geometrical parameters that can have the ideal mechanical properties.

Go Yamamoto, Yi Xiang, Koji Shimoyama, Keiichi Shirasu

## SIMULATION METHODS

To analyze the fracture process of MWCNTs and investigate the influence of their structural parameters/properties on their mechanical properties, uniaxial tensile loading tests were performed based on the MD method using the open-source software Large-Scale Atomic/Molecular Massively Parallel Simulator (LAMMPS), which was developed by Sandia National Laboratories in the United States and released in March 2018. The adaptive intermolecular reactive empirical bond order (AIREBO) model was used for the MD simulation. Being the second-generation extension of the reactive empirical bond order potential function, the AIREBO potential function additionally considers the 12–6 Lennard-Jones potential to describe the interaction between nanotube walls, resulting from the long-range van der Waals force, thus making it suitable for calculating the potential energy of covalent bonds and the interatomic force in MWCNTs. Different combinations of diameter, number of walls, chirality, and crosslink density of the models were explored to obtain an optimal structure. In order to efficiently handle such high workload calculations, the entire computational process from model building and crosslink introduction to MD simulation and result determination was controlled in the high throughput molecular dynamics (HTMD) environment by Python programs and shell script algorithms. The details of the model preparation and optimization procedures can be found in the literature [8–10].

To include a wide range of models, we investigated SWCNTs, 2-walled CNTs (2WCNTs), 3-walled CNTs (3WCNTs), 4-walled CNTs (4WCNTs), 5-walled CNTs (5WCNTs), 6-walled CNTs (6WCNTs), 7-walled CNTs (7WCNTs), and 8-walled CNTs (8WCNTs) with fixed lengths of 426.0 Å and 425.5 Å for zigzag and armchair CNTs, respectively. In order to make a valid comparison, the boundary of the diameters of the zigzag and armchair CNTs were assigned equal values. According to the diameters of (21,0) zigzag CNTs and (12,12) armchair CNTs (16.4 Å and 16.3 Å, respectively) and the diameters of (95,0) zigzag CNTs and (55,55) armchair CNTs (74.4 Å and 74.6 Å, respectively), the inner diameters of all CNT models were set in the range of 16.3 Å–74.6 Å. All MWCNTs were introduced via Frenkel-pair crosslinks by controlling the density, where the crosslink density is the number of crosslinks between two adjacent walls divided by the total number of atoms in the two walls. In the results reported by Byrne et al. [11], the 2WCNT models exhibited a "clean break" type fracture pattern when the crosslink density between the walls reached 2.5%. Based on this, in the present study, we set the crosslink density of our models in the range of 0–3%. In the Python-based HTMD platform, the CNT models were first generated with the desired diameter, number of walls, chirality, and crosslink density, and then the models were populated with randomly distributed crosslinks. The advantage of this method is that the time required to complete the modeling process depends on the number of atoms in the model.

To ensure equilibration of internal stresses and to minimize the total energy for each model, an isothermal-isobaric (NPT) ensemble was coupled to a nose-hoover thermostat and the relaxation process was performed under the following conditions: 300 K temperature, 0 applied load, and 0.5 fs time step. During the equilibrium period, the maximum and minimum AIREBO potential cutoff distances were set to 1.7 Å and 1.8 Å, respectively, to allow for better crosslink bonding. To avoid the influence of thermal fluctuations on the simulation results, the temperature was reduced to 1 K after obtaining the optimized model structure. Based on the experimental settings of the previous studies [12,13], the uniaxial tensile load was applied to the atoms of the two fixed parts of the outermost wall in the canonical ensembles (NVT) along the z-axis, with the engineering strain rate controlled at $6 \times 10^9$ S$^{-1}$ and the time step at 0.5 fs. Note that the fixed part also stretched along the tube axis as the load increased, while all the atoms in the mobile part, including the middle portion of the outermost wall and all the inner walls, were free to move, as shown in Fig 1. To avoid non-physical increases in stress values during tensile loading, the AIREBO potential cutoff distance was modified to 2.0 Å. The resultant tensile strength of the AIREBO potential-based tensile test verification simulation of the zigzag-type CNTs obtained in this study was 120 GPa. This was slightly higher than the experimental result, and consistent with those of the quantum calculation obtained by Peng et al. [5], which were approximately 100 GPa and 120 GPa. Moreover, the strain-stress relation for single-walled fracture of MWCNTs was in good agreement with their experiment sample 1, 2 and 3. Because the distribution pattern of the crosslinks may influence the result and the interwall crosslink density has at most 3% margin of error after equilibration, five calculations were performed for each MWCNT model, and the average values were considered to be the final results.
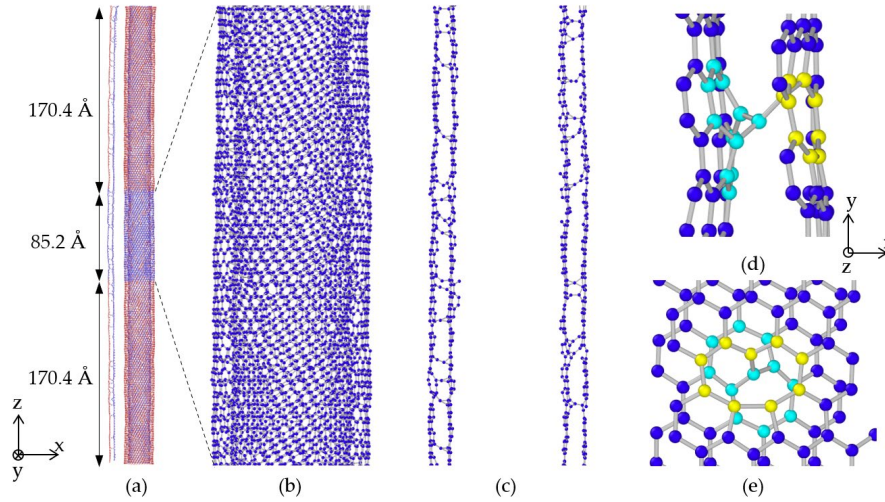
Figure 1: Schematic of the computational model. (a) Whole 2WCNT with Frenkel-pair crosslinks and distortions on the wall, with a half front slice on the left side, where the two red parts (on the outermost wall) indicate the regions of load application during the tensile test and are called fixed parts. The blue color (including all inner walls) represents the parts where atoms can move freely and are therefore called mobile parts; (b) magnified view of the middle mobile part of 2WCNT; (c) front slice from (b) showing randomly distributed crosslinks; (d),(e) structure of the Frenkel-pair crosslink. Light blue spheres represent carbon atoms on the inner walls and yellow spheres are atoms on the outer walls.

For each model, the values of strain, stress, nominal tensile strength, and nominal Young's modulus were obtained. The deformation along the z-axis of the model was divided by its original length to obtain the strain, and the stress was determined by dividing the stress tensor by the volume of carbon atoms, where the stress tensor was obtained using LAMMPS. The nominal tensile strength was calculated by dividing the product of the ultimate stress and the effective area by the total cross-sectional area. The effective area is the cross-sectional area under tensile stress, including the wall thickness of the model, as shown in Eq. (1), and the nominal area is the total cross-sectional area of the outermost wall, including the wall thickness, as shown in Eq. (2):

$$A_{\text{eff}} = \pi[(r_{\text{out}} + 0.5t)^2 - (r_{\text{in}} - 0.5t)^2], \tag{1}$$

$$A_{\text{nom}} = \pi(r_{\text{out}} + 0.5t)^2, \tag{2}$$

where $A_{\text{eff}}$ and $A_{\text{nom}}$ are the effective area and the nominal area, respectively; $r_{\text{in}}$ and $r_{\text{out}}$ are the radii of the innermost wall and outermost wall, respectively; and $t$ is the wall thickness. The nominal Young's modulus was calculated by dividing the nominal stress by the strain during elastic stretching. When calculating the area, the thickness of the individual wall was considered to be 3.4 Å.

As suggested in previous studies, we focused on structural optimization, particularly with respect to the nominal tensile strength. To optimize the structural parameters/properties for CNTs, a machine learning algorithm, namely the Bayesian optimization method, was used. A flowchart of this algorithm is shown in Fig. 2(a). Three basic steps were included in the Bayesian optimization adopted in this study: The first step involves the construction of the objective function using the Kriging model and the prediction of the optimal nominal tensile strength value based on the acquisition function by evaluating the expected improvement. In the second step, a genetic algorithm (GA) was introduced to determine the structural parameters/properties for the CNTs, that can achieve the predicted mechanical property, as shown in Fig. 2(b). Specifically, 1000 samples structured with randomly selected structural parameters/properties, including diameter, number of walls, chirality, and crosslink density, were generated as the population for the 1st generation; then the solution (nominal tensile strength) of each sample was calculated based on the objective function predicted by the Kriging model from the previous step. To determine the fitness parameter in the GA, the Michalewicz fitness function was used, and the solutions in the population were ranked in the objective function space using the Fonseca-Fleming method. The fitness was then assigned to each solution based on its rank. Using the stochastic universal

sampling method, better solutions were selected as parents to produce the next generation. During this process, blend crossover was performed with a crossover rate of 1.0, and uniform mutation was used with a mutation rate of 0.2. The process was repeated for 1000 generations, and an optimal structure with a set of structural parameters/properties was returned as the result of the GA. In the third step, the optimal structure was evaluated by the MD simulation to obtain the real nominal tensile strength value. This value, along with the structural parameters/properties, was then added to the data set as a new model. By repeating steps one to three, the structural parameters/properties were gradually optimized as the predicted parameters for the new model approached stability. In terms of computational cost, 250× 5 sets of models with structural parameters/properties were considered as the initial database.
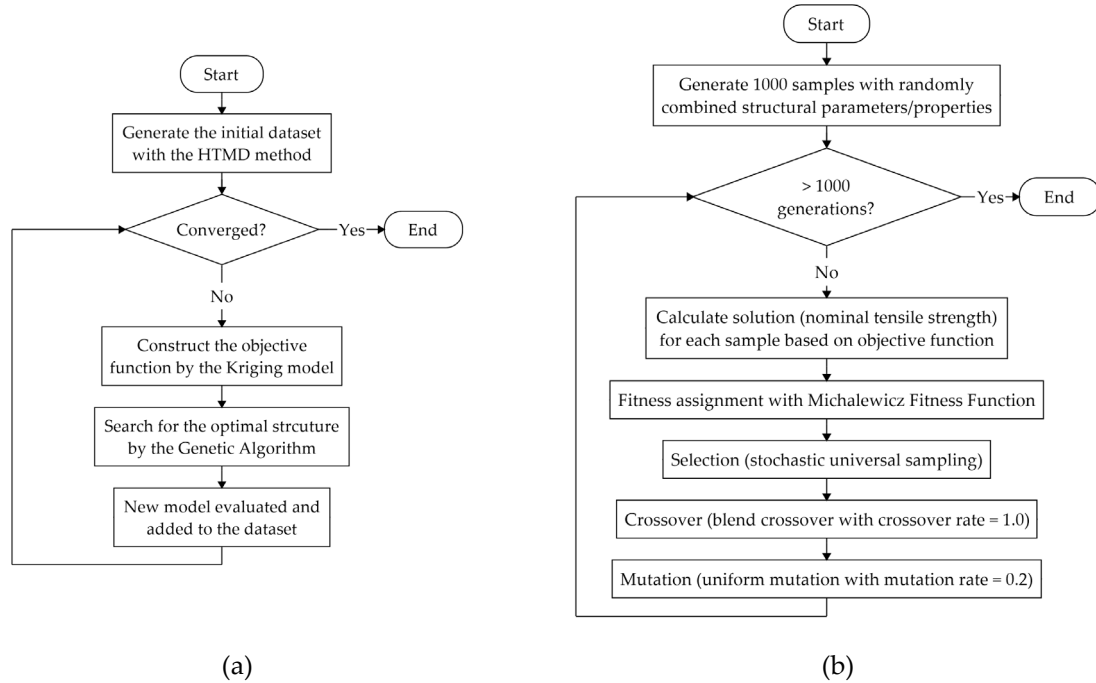


(a)                                                                 (b)

Figure 2: Flowchart of the optimization procedure. (a) Bayesian optimization; (b) genetic algorithm.

## RESULTS

For all results, the error in nominal tensile strength was less than 5%, due to the error in both crosslink density and crosslink distribution difference. Based on our calculations, the structure optimization was performed 52 times. The tensile strength results for each predicted model are shown in Fig. 3, and their representative values are listed in Table 1. It can be observed that there are fluctuations in the initial prediction results; with the repetition of the prediction procedure, the tensile strength of the newly predicted structure tends to stabilize. However, the values in Table 1 show that although the chirality, number of walls, and diameter become stable, the predictions of the crosslink density for each adjacent wall continue to fluctuate. This is due to the influence of crosslink distributions and the presence of margin errors. Therefore, we combined the prediction models corresponding to the 10 highest tensile strength values as the final result. The armchair-type 8WCNT was concluded to be the optimal structure with high mechanical performance, where the inner diameter was 10.9 Å; the crosslink densities between the adjacent walls from the inner to outer tubes were 1.01%, 0.93%, 1.14%, 0.92%, 0.84%, 1.08%, and 1.19%; and the nominal tensile strength and nominal Young's modulus values were approximately 57–59 GPa and 650–670 GPa, respectively. The effective tensile strength and Young's modulus values based on the effective cross-sectional area (Eq. 1) were slightly higher than nominal values and range from approximately 64–65 GPa and 701–724 GPa, respectively.
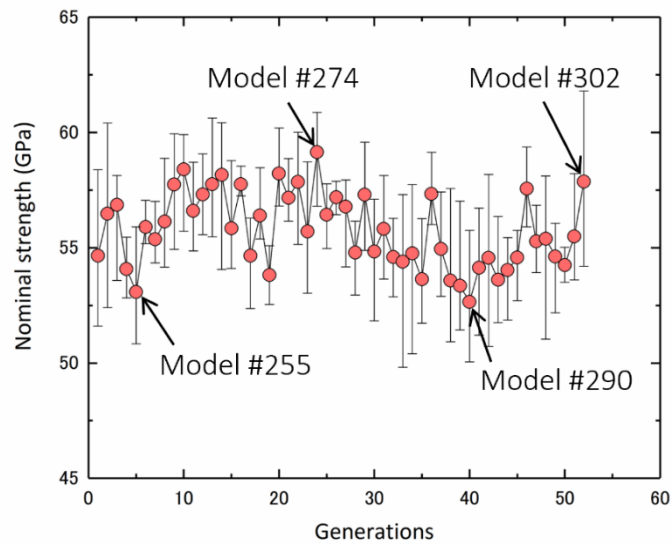
Figure 3: Strength results of the machine learning-predicted structure with respect to the repetition of the prediction procedure. Error bar shows the maximum and minimum values obtained from the three repetitions of calculations.

Table 1: Detailed information for the representative values in Figure 3. "Crosslink density 1" through "Crosslink density 7" represent the crosslink densities between each adjacent wall from the inner tube to the outer tube. The average value is given, and the range is indicated in parentheses.

| Model | Inner diameter (Å) | Number of walls | Chirality | Crosslink density 1 (%) | Crosslink density 2 (%) | Crosslink density 3 (%) | Crosslink density 4 (%) | Crosslink density 5 (%) | Crosslink density 6 (%) | Crosslink density 7 (%) | Nominal strength (GPa) |
|---|---|---|---|---|---|---|---|---|---|---|---|
| 255 | 13.6 [10,10] | 8 | Armchair | 1.23 (1.21-1.25) | 0.06 (0.06-0.07) | 0.45 (0.44-0.46) | 0.79 (0.78-0.80) | 0.75 (0.72-0.77) | 1.15 (1.11-1.17) | 1.03 (1.02-1.04) | 53.08 (50.84-55.90) |
| 274 | 10.9 [8,8] | 8 | Armchair | 1.12 (1.11-1.14) | 0.84 (0.83-0.87) | 1.21 (1.19-1.23) | 1.31 (1.27-1.34) | 1.28 (1.26-1.30) | 0.85 (0.82-0.87) | 1.18 (1.16-1.19) | 59.15 (56.79-60.87) |
| 290 | 10.9 [8,8] | 8 | Armchair | 0.45 (0.38-0.42) | 1.23 (1.19-1.25) | 2.01 (2.00-2.03) | 0.19 (0.18-0.20) | 0.52 (0.50-0.52) | 0.95 (0.93-0.98) | 0.92 (0.89-0.93) | 52.65 (50.05-55.75) |
| 302 | 10.9 [8,8] | 8 | Armchair | 0.97 (0.94-1.02) | 0.93 (0.91-0.94) | 1.12 (1.09-1.15) | 0.90 (0.87-0.92) | 0.82 (0.80-0.82) | 1.07 (1.06-1.09) | 1.18 (1.17-1.18) | 57.87 (54.20-61.80) |

## CONCLUSIONS

We presented a novel approach to predict the optimal structure of high-mechanical performance CNTs through machine learning-based simulations in the HTMD environment. Based on the results obtained for the structural parameters/properties of diameter, number of walls, chirality, and crosslink density, we concluded that to achieve a high nominal tensile strength, armchair-type MWCNTs with the smallest diameter, large number of walls, and a suitable crosslink density between the adjacent walls are preferred. Based on our calculations, the armchair type 8WCNT with the inner diameter of 10.9 Å, the crosslink density between adjacent walls (from inner tube to outer tube) of 1.01%, 0.93%, 1.14%, 0.92%, 0.84%, 1.08%, and 1.19% has the best mechanical properties. The nominal tensile strength, nominal Young's modulus, effective tensile strength, and effective Young's modulus were approximately 57–59 GPa, 650–670 GPa, 64–65 GPa, and 701–724 GPa, respectively. We further discussed the relationship between fracture pattern and mechanical properties of CNTs, and it was observed that the tubes with "near-clean-break" fracture mode and "clean-break" fracture mode tended to exhibit high tensile strength. We explained the reason behind the specific structural parameters/properties that facilitate high mechanical performance, and showed that the influence of crosslink density on mechanical properties has a tendency to gradually decrease from the outer walls to the inner walls. The proposed method and the obtained results presented a valuable approach to understand the mechanical properties of CNTs and provided guidance for tailoring CNT structures to improve the quality of composites.

Go Yamamoto, Yi Xiang, Koji Shimoyama, Keiichi Shirasu

## ACKNOWLEDGEMENTS

## REFERENCES

[1]     Y. Shimamura, K. Oshima, K. Tohgo, T. Fujii, K. Shirasu, G. Yamamoto, T. Hashida, K. Goto, T. Ogasawara, K. Naito, T. Nakano and Y. Inoue, Tensile mechanical properties of carbon nanotube/epoxy composite fabricated by pultrusion of carbon nanotube spun yarn preform, *Composites: Part A*, **62**, 2014, pp. 32–38 (doi: 10.1016/j.compositesa.2014.03.011).

[2]     G. Yamamoto, K. Shirasu, Y. Nozaka, W. Wang, T. Hashida, Microstructure-property relationships in pressureless-sintered carbon nanotube/alumina composites, *Materials Science & Engineering A*, **617**, 2014, pp. 179–186 (doi: 10.1016/j.msea.2014.08.068).

[3]     W. Wang, G. Yamamoto, K. Shirasu, Y. Nozaka and T. Hashida, Effects of processing conditions on microstructure, electrical conductivity and mechanical properties of MWCNT/alumina composites prepared by flocculation, *Journal of the European Ceramic Society*, **35**, 2015, pp. 3903–3908 (doi: 10.1016/j.jeurceramsoc.2015.06.027).

[4]     M.F. Yu, O. Lourie, M.J. Dyer, K. Moloni, T.F. Kelly and R.S. Ruoff, Strength and breaking mechanism of multiwalled carbon nanotubes under tensile load, *Science*, **287**(5453), 2000, pp. 637–640 (doi; 10.1126/science.287.5453.637).

[5]     B. Peng, M. Locascio, P. Zapol, S. Li, S.L. Mielke, G.C. Schatz and H.D. Espinosa, Measurements of near-ultimate strength for multiwalled carbon nanotubes and irradiation-induced crosslinking improvements, *Nature nanotechnology*, **3**(10), 2008, pp. 626–631 (doi: 10.1038/nnano.2008.211).

[6]     G. Yamamoto, K. Shirasu, Y. Nozaka, Y. Sato, T. Takagi and T. Hashida, Structure-property relationships in thermally-annealed multi-walled carbon nanotubes, *Carbon*, **66**, 2014, pp. 219–226 (doi; 10.1016/j.carbon.2013.08.061).

[7]     K. Shirasu, G. Yamamoto and T. Hashida, How do the mechanical properties of carbon nanotubes increase? An experimental evaluation and modelling of the engineering tensile strength of individual carbon nanotubes, *Materials Research Express*, **6**(5), 2019, Article number 055047 (doi: 10.1088/2053-1591/ab069f).

[8]     Y. Xiang, K. Shimoyama, K. Shirasu and G. Yamamoto, Machine learning-assisted high-throughput molecular dynamics simulation of high-mechanical performance carbon nanotube structure, *Nanomaterials*, **10**(12), 2020, pp. 1–13 (doi: 10.3390/nano10122459).

[9]     Y. Xiang and G. Yamamoto, A data mining approach to investigate the carbon nanotubes mechanical properties via high-throughput molecular simulation, *Materials Science Forum*, **1023**, 2021, pp. 29–36 (doi: 10.4028/www.scientific.net/MSF.1023.29).

[10]    G. Yamamoto, Y. Chen, A. Kunitomo, N. Shigemitsu and T. Shindo, Decreasing vacancy-defect sensitivity in multi-walled carbon nanotubes through interwall coupling, *Carbon Trends*, **11**, 2023, Article number 100266 (doi: 10.1016/j.cartre.2023.100266).

[11]    E.M. Byrne, M.A. McCarthy, Z. Xia and W.A. Curtin, Multiwall nanotubes can be stronger than single wall nanotubes and implications for nanocomposite design, *Physical Review Letters*, **103**(4), 2009, Article number 045502 (doi: 10.1103/PhysRevLett.103.045502).

[12]    G. Yamamoto, J.W. Suk, J. An, R.D. Piner, T. Hashida, T. Takagi and R.S. Ruoff, The influence of nanoscale defects on the fracture of multi-walled carbon nanotubes under tensile loading, *Diamond & Related Materials*, **19**, 2010, pp. 748–751 (doi: 10.1016/j.diamond.2010.01.045).

[13]    G. Yamamoto, K. Shirasu, T. Hashida, T. Takagi, J.W. Suk, J. An, R.D. Piner and R.S. Ruoff, Nanotube fracture during the failure of carbon nanotube/alumina composites, *Carbon*, 49, 2011, pp. 3709–3716 (doi: 10.1016/j.carbon.2011.04.022).